EFFECT OF WETTABILITY ON THE PETROPHYSICAL PARAMETERS OF VUGGY CARBONATES: NETWORK MODELING INVESTIGATION

S. Békri, C. Nardi, O. Vizika
Institut Français du Pétrole, 1 et 4 avenue de Bois-Préau,92852 Rueil-Malmaison, France

This paper was prepared for presentation at the International Symposium of the Society of Core Analysts held in Abu Dhabi, UAE, 5-9 October, 2004

ABSTRACT

Carbonate rocks often present bimodal pore size distributions usually attributed to the presence of vugs that can communicate through the matrix (separated vugs) or form an interconnected pore system (touching vugs). Due to these different degrees of interconnectivity, vugs and matrix may have different wettability, with the matrix being usually water-wet and the vugs oil-wet. These wettability heterogeneities and connectivity regimes infer to the porous medium petrophysical properties that may vary within a wide range of values. The objective of the present work is to demonstrate the effect of pore-scale wettability heterogeneities on effective capillary pressure and relative permeability values of vuggy structures.

To this end a pore network numerical simulator is used, that calculates multiphase flow properties taking into account the bimodal pore structure specificity and the fractional wettability. The complex real pore space is represented as a dual-network model that incorporates information on the primary (matrix) and the secondary (vugs, fractures) porosity and accounts for the connectivity of the secondary porosity. The model permits to impose heterogeneous wettability by assigning different water/oil contact angles according to the desired heterogeneity pattern. In water/oil displacements, drainage and imbibition mechanisms occur simultaneously according to the local wettability.

INTRODUCTION

Heterogeneous wettability at local scale is very frequent in carbonate reservoirs and may drastically affect the macroscopic characteristics and transport properties. Wettability heterogeneities may be related to heterogeneous permeability, which is known to play a determining role on the flow properties. The objective of the present paper is to study the impact of the small-scale wettability heterogeneities on two-phase capillary pressure and relative permeability of dual-porosity structures through a pore scale modelling approach. The results give valuable insight in the different parameters determining the transport properties of vuggy or fractured carbonate rocks.

Network modelling has proved to be a powerful tool for predicting average multiphase flow properties such as relative permeability and capillary pressure. In these models the pore space of the homogeneous (or single porosity) rocks is represented by an equivalent network of interconnected pores. An extension to dual-porosity rocks has also been looked at more recently (Békri et al. [1] and Ioannidis et al. [10]).

The dual-porosity structures characterised by a primary (or matrix) porosity and a secondary porosity consisting of vugs and fractures are modelled by a dual-network which incorporates information on the different porosities. The interconnectivity of these coexisting networks, that can have different wettabilities, is a major issue, that severely affects fluid distributions within the pore space and consequently all related petrophysical properties.

The effect of wettability on two-phase flow of homogeneous media (single porosity) has first been looked at by Heiba et al. [2], and more recently by McDougall and Sorbie [4, 5], Blunt [6] and Oren et al [7]. The wettability of the pore walls may turn to oil-wet by absorption of hydrophobic components (Kovscek et al. [8]) in the pores contacted by the oil phase. Waterfloods were simulated also in mixed-wet systems. Mixed or fractional wettability refers to distinct and separate water-wet and oil-wet surfaces that coexist in the porous medium. It has been shown that wettability distribution affects waterflooding efficiency and/or relative permeability.

In the present work a pore network numerical simulator is used, that calculates multiphase flow properties taking into account the bimodal pore structure specificity and the fractional wettability. The pore space is represented as a dual-network model that incorporates permeability and wettability heterogeneities.

In the first part of the paper, the three-dimensional dual pore-network is described. In the second part of the paper, the numerical results are presented: two-phase capillary pressure and relative permeabilities are calculated using dual networks of different wettability. For that purpose, two-phase capillary-controlled displacement processes are simulated. When the two phases are oil and water, the displacement is influenced by the local wettability.

After a primary drainage displacement the oil phase was assumed directly in contact with the solid surface of the vugs. The wettability of the vugs surface is supposed to be altered due to surface active components deposition.

In the present work it is assumed that the well-connected macropores of the medium are strongly oil-wet. The behaviour for varying oil/water contact angle of the micropores (matrix) has been studied. Using dual porosity network modeling the effect of permeability and wettability contrast between matrix and vugs on the capillary pressure and oil/water relative permeability curves has been evaluated.

MODELING

The dual network modeling consists in two stages. In the first stage the matrix is modeled using single porosity network modeling and its average macroscopic properties (capillary

pressure and relative permeability) are calculated. In the second stage the vugs are treated in a discrete form (considered as forming a network) while the matrix is taken into account through the macroscopic properties (capillary pressure and relative permeabilities as a function of saturation: Kr(S), Pc(S)).

As a sample case the carbonate rock with bimodal porosity structure consisting of a fine-grained matrix and both well-connected and isolated (communicating through the matrix) macropores used in Moctezuma et al. [11] was used in this study. Its total porosity is 33.8% and the permeability 115 mD. Figure 1 presents the mercury porosimetry data and NMR spectra of the rock. The methodology used to extract data on the porous medium structure that will be used to construct a pore network model representative of a double porosity rock is described in Moctezuma et al. [11]. This method consists in acquiring mercury porosimetry data and NMR spectra of the rock, at various well-determined water saturations. Combination of these two informations gives consistent pore-size distributions and pore/pore-throat correlations of the micro- and macro-pore structure.

The detailed pore size distributions of each system (micro-, macro-pores) have been used to construct an adapted dual porosity network model (Békri et al. [1]). First the matrix properties, $Pc_m(S_w)$ and $Kr_m(S_w)$, are generated using a single porosity network model. Then the properties of the well-connected macropores are reproduced to construct the network that is finally coupled to the matrix using the dual porosity option.

Single Porosity Network Model

The network model is a conceptual representation of a porous medium. The pore structure is modelled as a bi or three-dimensional network of narrow channels interconnecting pores. A real porous medium is characterised by surface roughness and angles, through which the wetting phase remains continuous and flows simultaneously with the non-wetting phase occupying the bulk of the pores. To take into account this displacement mechanism, pores and pore-throats are considered to have angular sections. The channels (pore-throats) have triangular cross-section and variable length. The pores are simulated as cubes. Each pore is accessible by six identical channels. An equivalent diameter D_p and d_c for the pores and the channels is associated to the geometry. A schematic depiction of a unit cell is given in Figure 2. L represents the characteristic length of the network that corresponds to the distance between two adjacent nodes (center of the pores). When L is defined, the macroscopic properties of porosity, permeability, capillary pressure and relative permeability can be calculated. A more detailed description of the model can be found in Laroche [15] along with a long list of references on this type of models.

Network Model for the Matrix and the Well-connected Macropores

Ideally, the network model is generated based on the pore and throat distributions and their correlation. Using the methodology described in Moctezuma et al. [11], the pore and throat distributions can be obtained independently but not, for the moment, their correlation. The models constructed using measured pore and throat size distributions have to be calibrated

so that they respect the properties measured in the laboratory: mercury injection capillary pressure, porosity and permeability.

Volumes for throats and pores are assumed to be proportional to their inscribed diameters d_c and D_p to a certain exponent, λ_c and λ_p respectively, following the relationships $V_c(d) \sim d^{\lambda c}$ and $V_p(D) \sim D^{\lambda p}$. This empirical approach has been used by many authors to represent the relationship between radius and volume for real pores (Heiba et al. [3] and Fenwick at al. [12]). The prefactors in the previous relationships are given by:

$$V_p\left(D_p\right) = c_p \overline{D}_p^{\left(3-\lambda_p\right)} D_p^{\lambda_p} \tag{1}$$

$$V_c\left(d_c\right) = c_c\left(L - \overline{D}_p\right)\overline{d}_c^{\left(2-\lambda_c\right)} d_c^{\lambda_c} \tag{2}$$

where c_p and c_c are constants. For the different combinations of λ_p, λ_c, c_p, c_c and L it is possible to construct different networks with specific properties. The used throat-size frequency (throat-size distribution) and the pore-size frequency are given in Figure 3. In order to respect this distribution an arbitrary correlation between pore and throat is used. It consist to associate the smallest pore to the smallest throat of the measured frequency. The parameters that are tuned to reproduce the experimental porosity and permeability are L, c_c, c_p, λ_c and λ_p. All the parameters and the properties obtained for the matrix and the dual network are summarized in Table 1.

From mercury injection it is found that the porosity fraction for the matrix is 0.48 corresponding to a porosity of 22.13% in the bimodal structure. Due to the fact that it is not possible to measure independently the matrix permeability, estimation is made considering an average value of the pore-throat radii from the mercury injection in the zone of micropores. This average pore throat radius is 0.05 μm. Applying the capillary tube model $K = r^2 \Phi / 8$ (Dullien, [9]) the permeability of the matrix is estimated at about 0.1 mD.

To construct the pore network medium, a set of pores was randomly generated based on a given pore size distribution (cf. Figure 3.a). The throats interconnecting pores are also randomly generated based on the given distribution (cf. Figure 3.a) with the only constraint that d_c is smaller than D_p. In order to model the flow of the wetting phase, the asperities and roughness of the surface of the rocks were taken in account, pore shape is considered to be angular (triangular and square cross-sections respectively for pore-throats and pore-bodies). The throats form 45 degree angles to the flow direction in the horizontal plane. Periodic boundary conditions are used in the directions perpendicular to the inlet/outlet direction to minimise finite size effects. Figure 3.b presents the comparison of the experimental throat-size and pore-size frequency to the generated ones. The agreement is very satisfactory.

Figure 4 presents water/oil capillary pressure and relative permeabilities for water injection (forced imbibition) for the matrix and the well-connected macropores when both are oil-wet. In order to compare the characteristics of the micro- and macro- structure, the relative permeabilities of both structures are normalized to the mean absolute permeability of the core (115mD). The relative permeabilities and the capillary pressure curves are given as

function of the total saturation (Sw') in the dual porosity structure. Sw' from 0 to 43% correspond to the macropores and Sw' from 43% to 100% correspond to the micropores.

Dual Porosity Network Model

The dual-porosity network model approach is applied at two scales as illustrated in Figure 5a. The dual porosity model combines transport properties data of the matrix (capillary pressure and relative permeabilities considered as homogeneous) with the explicit simulation of flow in the well-connected macropores network (vugs).

The bimodal porous medium is characterized by a bimodal pore-throat radii distribution. The NMR pore distribution is used to build a three-dimensional lattice of pores and throats representing the secondary porosity. These pores and throats are surrounded by a matrix with known properties (porosity, absolute permeability, capillary pressure and relative permeability). Matrix permeability K_m and porosity Φ_m may be spatially distributed within the 3-D lattice. In this paper, it is assumed for simplicity that matrix properties are uniform.

The primary drainage in water-wet conditions (or forced imbibition in oil-wet) in dual-porosity rocks is simulated using invasion percolation for the simple porosity model (Killins et al. [14]) with the following modification. The capillary pressure P_c^t required for the non-wetting phase invasion into a given throat may be determined by either its minimum radius r, or the capillary pressure of the matrix Pc_m. This may be expressed as

$$Pc^t = min[Pc(r), Pc_m] \quad (3)$$

where $Pc(r)$ is the threshold pressure of the throat of the well-connected macropores. When the pressure exceeds Pc_m, the matrix will be invaded by the non-wetting phase.

The global porosity Φ of such dual-network is calculated from the primary Φ_m and secondary porosity Φ_M:

$$\Phi = \Phi_M + \Phi_m.(1- \Phi_M) \quad (4)$$

Similarly, conductance g^α and non-wetting phase saturation S_{nw} are calculated for each applied capillary pressure, P_c, knowing the matrix capillary pressure and relative permeability functions (from which the matrix conductance $g^\alpha_m(S_{nwm}(P_c))$ is deduced from the single porosity model):

$$\Phi.Snw = \Phi_M.Snw_M + \Phi_m.(1- \Phi_s).S_{nwm}(P_c) \quad (5)$$

$$g^\alpha = g^\alpha_M + g^\alpha_m(S_{nwm}(P_c)) \quad (6)$$

where S_{nws}, g^α_M are non-wetting phase saturation and conductance of the secondary porosity, calculated using the classical approach of pore network simulation.

Knowing the conductivity of each phase one calculates the permeability and the relative permeabilities in the same way as for the single porosity model.

Figure 5.b presents forced imbibition water/oil relative permeabilities for the dual-network, where matrix and the well-connected macropores are strongly oil wet (i.e. the advancing

oil/water contact angle for waterflooding, θ_{aw_Ma}, is equal to 180°). The shape of the oil relative permeability is controlled by both macro- and micro- pores structure. The crossing point (Krw=Kro) is located at low water saturation (Sw=17%). This is attributed to the oil wettability and to the bimodal pore structure (early water breakthrough through the interconnected vuggy structure). This phenomenon, often observed in experimental coreflooding, is in general qualitatively attributed to core sample heterogeneity. It is clearly shown here that it can be due to small scale heterogeneity (bimodal structure) and that it could be quantitatively related to it.

RESULTS

The total porosity and global permeability were matched to 33.8% and 115 mD respectively (the experimental values). All two phase simulations were performed with an oil-wet condition for the well-connected macropores (θ_{aw_Ma} = 180°). The wettability of the micropores (matrix) is varying from oil-wet to intermediate-wet (θ_{aw_Mi} from 180° to 90°).

Figures 4 and 5.b show the relative permeabilities and the capillary pressure for the matrix, the vugs and the dual porosity model as function of normalized saturation (Sw'). The relative permeabilities were obtained by normalization to the mean absolute permeability of the core (115mD), and the saturation represents the total saturation in the dual porosity structure. The saturation in each pore structure was multiplied by the respective pore volume fraction (43% for the vugs, 57% for the matrix) so that both micro- and macrostructure relative permeability curves are presented next to each other in Figure 4b.

When both micro and macropores are strongly oil-wet, Figure 5.b shows that oil relative permeability is strongly affected by the matrix, while water relative permeability is controlled by the vuggy system. At the beginning of water injection the relative permeability to oil is mainly controlled by the vuggy system, then when the water invades most of the big vugs oil flows essentially through the matrix, and its relative permeability is controlled by the matrix characteristics. Since water is the injected phase and also strongly non-wetting, its relative permeability is exclusively dominated by the vuggy system characteristics.

Figure 6 shows the oil and water relative permeabilities and capillary pressure for water injection for θ_{aw_Mi} = 180° (case 1), θ_{aw_Mi} = 95° (case 2), θ_{aw_Mi} = 94° (case 3) and θ_{aw_Mi} = 90° (case 4). For case 1, the water invades the well-connected macropores first and then the micropores. In the opposite, for case 4, the water preferentially invades the micropores, resulting, for the same saturation level as in case 1, in a higher oil permeability and lower water permeability. The simulations clearly demonstrate the effect of the matrix/vugs wettability contrast on the effective capillary pressure. When matrix and vugs are both strongly oil-wet, the water/oil capillary pressure follows exactly the mercury Pc curve and reflects the permeability contrast. Wettability heterogeneities can attenuate the capillary pressure threshold contrast and make the Pc curves shrink. Relative permeability values are also strongly affected by wettability heterogeneities in vuggy structures. The wettability pattern favors flow of one of the two phases in the high permeability interconnected

pathway formed by the vugs. This phase has high relative permeability to the detriment of the other phase mobility.

Three simulations of waterflooding were performed to investigate the effect of various permeability contrasts between macro and micropores. Matrix permeability values of 1, 10 and 100 times the initial value K_{m0} were taken. The capillary pressure curve of the matrix was adjusted to the chosen permeability by dividing the initial values of the capillary pressure by a factor $\sqrt{K_m/K_{m0}}$.

The effect of the matrix transport properties on a dual-porosity system is illustrated in Figure 7. It shows the global water-oil relative permeability and capillary pressure behavior for different matrix permeability values. The macropores are always oil-wet. The matrix is either strongly oil-wet or moderately oil-wet. The matrix first invasion is related to its permeability value, i.e. its threshold radius. For $K_m/K_{m0}=1$ (i.e. $K_M/K_m=1200$) invasion in the matrix starts only when network invasion is completed, while for $K_m/K_{m0}=10$ and 100 (i.e. $K_M/K_m=120$ and $K_M/K_m=12$) invasion in matrix starts before the network is completely invaded; for $K_m/K_{m0}=100$ (with $\theta_{aw\_Mi}=100$) invasion of the matrix starts shortly after starting of the secondary network invasion, and progresses in parallel in both pore systems. This behavior in terms of pore space occupation by the different phases is reflected on the relative permeability curves. It is observed that the non-wetting phase (water) relative permeability increases dramatically with increasing contrast between primary and secondary network permeability (i.e. case where $K_m/K_{m0}=1$), showing that existence of highly connected pathways of vugs enhances non-wetting phase mobility, while wetting phase mobility (oil) is decreased.

Water (non-wetting phase) relative permeability decreases as the contrast between vugs and matrix permeability decreases, while at the same time the oil (wetting phase) permeability increases. A wettability contrast between macropores (oil-wet) and matrix (moderately oil-wet) favors always oil (wetting phase) mobility while water relative permeability goes down very rapidly.

CONCLUSIONS

A dual network model for dual porosity rocks was presented. The model incorporates information on the primary (matrix) and the secondary (vugs, fractures) porosity. It also accounts for limited or partial connectivity of the secondary porosity.

With this model a pore network has been constructed that satisfactorily reproduces the capillary pressure curve, the porosity and the permeability determined experimentally on a double porosity rock. Capillary pressures and relative permeabilities are calculated for various permeability contrasts between matrix and vugs/fractures and spatial wettability heterogeneity distributions.

The contrast between primary and secondary pore space characteristics has a major effect on both the capillary pressure and the relative permeabilities. It was demonstrated that wetting phase relative permeability is, depending on its saturation, affected by both the vugs and the matrix characteristics, while the non-wetting phase is mainly controlled by

the vuggy system. High permeability contrasts between vugs and matrix favor non-wetting phase mobility.

The simulations clearly demonstrate the effect of the size and distribution of wettability heterogeneities on water/oil displacement. A wettability contrast between macropores (oil-wet) and matrix (moderately oil-wet) favors always oil (wetting phase) mobility while water (non-wetting phase) relative permeability decreases very rapidly. This result highlights also the importance of a correct wettability restoration on the reliability of the petrophysical parameters measurement. Unrealistic extreme oil-wet conditions in the matrix would lead to underestimation of the oil relative permeabilities.

NOMENCLATURE

D_p = pore diameter
$\overline{D}_p$ = average pore diameter
d_c = channel/throat diameter
$\overline{d}_c$ = average channel diameter
g = conductance
K = permeability
K_r = relative permeability
L = network length
P_C = capillary pressure
r = throat radius
S = saturation
S' = normalized saturation
V = volume
λ = exponent of the inscribed diameter related to the volume
θ_{aw} = advancing oil/water contact angle measured in water phase
ϕ = porosity

Subscripts
m = micropores
M = macropores
α, β = fluid in place
p = pore
c = channel
w,o = *water*, oil phase

REFERENCES

1. Békri S., C. Laroche and O. Vizika, "Pore-Network Models to Calculate Transport Properties in Homogeneous and Heterogeneous Porous Media", *XIV International Conference on Computational Methods in Water Resources*, Delft, The Netherlands, (2002), Jun 23-28.
2. Heiba A.A., H.T. Davis, L.E. Scriven, "Effect of wettability on two-phase relative permeabilities and capillary pressures", SPE12172, *presented at the SPE Annual Technical Conference and Exhibition*, Scan Francisco, CA, USA, (1983) October 5-8.
3. Heiba, A.A., M. Sahimi, L.E. Scriven and H.T. Davis, "Percolation theory of two-phase relative permeability", *SPE Reservoir Engineering*, (1992), **7**, 123-132
4. McDougall S.R., K.S. Sorbie, "The impact of wettability on waterflooding: pore-scale simulation". *SPE Reservoir Engineering*, (1995), 208-213.
5. McDougall S.R., K.S. Sorbie, "Application of network modelling techniques to multiphase flow in porous media", *Petroleum Geoscience*, (1997), **3**, 161-169.

6. Blunt M.J., "Pore level modelling of the effects of wettability", *SPEJ*, (1997), **2**, 494-510.
7. Oren P.E., S. Bakke, O.J. Arntzen, "Extending predictive capabilities to network models", SPE38880, *presented at the SPE Annual Technical Conference and Exhibition*, San Antonio, Texas, USA, (1997), October 5-8.
8. Kovscek A.R., H. Wong, C.J. Radke, "A pore-level scenario for the development of mixed wettability in oil reservoirs", *AIChE Journal*, (1993), **39** (6), 1072-1085.
9. Dullien F.A.L., "Porous Media", *Fluids Transport and Pore Structure*, Academic Press (1992).
10. Ioannidis M.A., I. Chatzis, "A Dual-Network Model of Pore Structure for Vuggy Carbonates", SCA2000-09, *International Symposium of the Society of Core Analysts*, Abu Dhabi, UAE, (2000), Oct.
11. Moctezuma A., S. Békri, C. Laroche, O. Vizika, "A dual network Model for relative permeability of bimodal rocks application in a vuggy carbonate", SCA2003-94, *International Symposium of the Society of Core Analysts*, Pau, France, (2003), Sept.
12. Fenwick D.H. and M.J. Blunt, "Three-dimensional modeling of three-phase imbibition and drainage", *Adv. Water Resources*, (1998), **21**(2), 121-143.
13. Kamath J., B. Xu, S.H. Lee and Y.C. Yortsos, "Use of Pore Network Models to Interpret Laboratory Experiments on Vugular Rocks", *Journal of Petroleum Science and Engineering*, (1998), **20**, 109-115.
14. Killins C.R., R.F. Nielsen, J.C. Calhoum, "Capillary Desaturation and imbibition in porous rocks", *Producers Monthly*, (1953), Dec., **18**(2), 30-39.
15. Laroche C., "Déplacements Triphasiques en Milieu Poreux de Mouillabilité Hétérogène", PhD Thesis, *Université de Paris XI*, Paris, (1998).
16. Laroche C., O. Vizika, F. Kalaydjian, "Network modeling as a tool to predict three-phase gas injection in heterogeneous wettability porous media", *Journal of Petroleum Science and Engineering*, (1999), **24**, 155-16.
17. Laroche C., "Capillary pressure and relative permeability curves in mixed-wet media using Network modeling", *Proceedings of the 6th International Symposium on Evaluation of Reservoir Wettability and its Effect on Oil Recovery*, Socorro, NM, USA (2000), 27-28 September.
18. Laroche C., O. Vizika, G. Hamon and R. Courtial, "Two-phase Flow Properties Prediction from Smale-Scale Data Using Pore-Network Modeling", SCA2001-16, *International Symposium of the Society of Core Analysts*, Edinburgh, U.K., (2001) Sept.
19. Vizika O. and R. Lenormand, "Flow by film of the wetting phase in a porous medium and its role on the gravity drainage process", *Presented at the IEA 12th International Workshop and Symposium*, Bath, UK, (1991), 28-30 October.
20. Lucia F. J., "Carbonate Reservoir Characterization", *Springer, (1999)*.
21. Tsakiroglou C.D., G.B. Kolonis, T.C. Roumeliotis and A.C. Payatakes, "Mercury Penetration and Snap-Off in Lenticular Pores", *J Colloid Interface Sci* , (1997), **193**(2), 259-272.
22. Xu B., J. Kamath, Y.C. Yortsos and S.H. Lee, "Use of Pore Network Models to Simulate Laboratory Corefloods in a Heterogeneous Carbonate Sample", *SPE J.*, (1999), **4** (3), Sept, 179-186.

Table 1. Geometrical parameters and calculations of porosity and permeability for the matrix and the well-connected macropores.

Parameters	Micropores	Macropores
$\overline{D}_p$	0.90 μm	688 μm
$\overline{d}_c$	0.41 μm	28 μm
L	2.245 μm	1215 μm
C_c	0.89	0.308
λc	2	2
C_p	0.89	0.308
λp	2	2
Φ	0.22	0.147
K	0.102 mD	114.7 mD

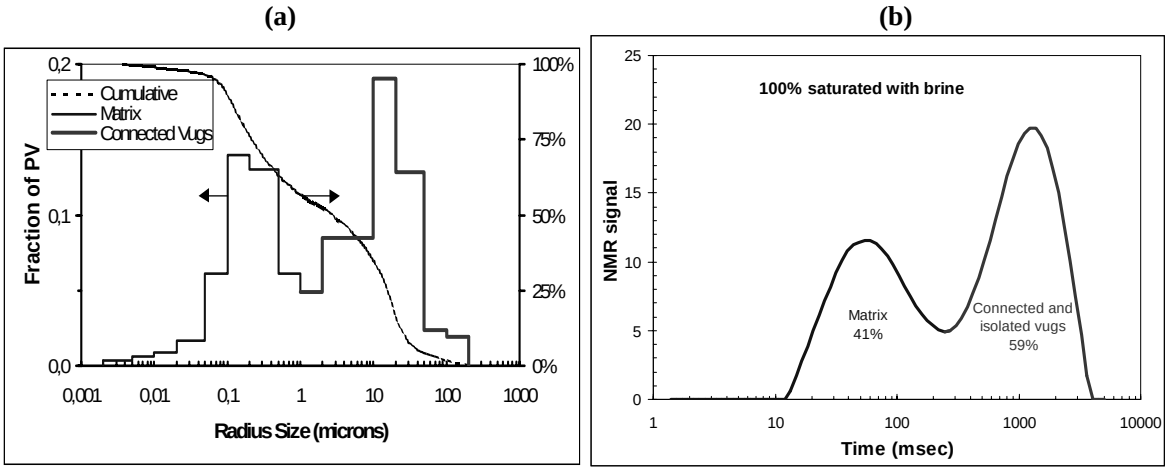

Figure 1. (a) Mercury porosimetry data and (b) NMR amplitude signal of the treated carbonate rock.

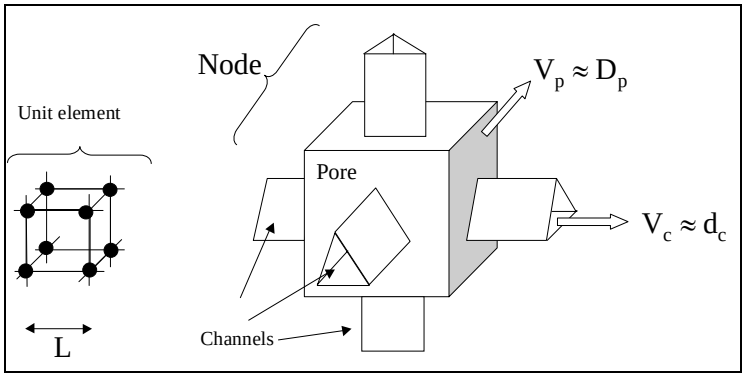

Figure 2. Schematic depiction of a unit cell of the network model (Laroche, 1998)

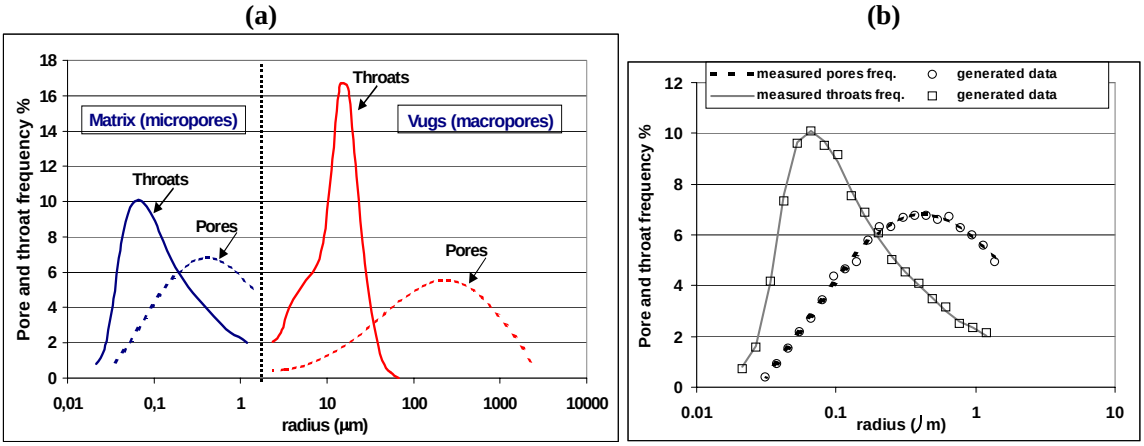

Figure 3. (a) Pore (dashed lines) and pore-throat (continuos lines) size frequency obtained for the micropores (matrix) and for the well-connected macropores as a function of the pore radius. (b) Comparison of the pore and pore-throat size frequency for the matrix.

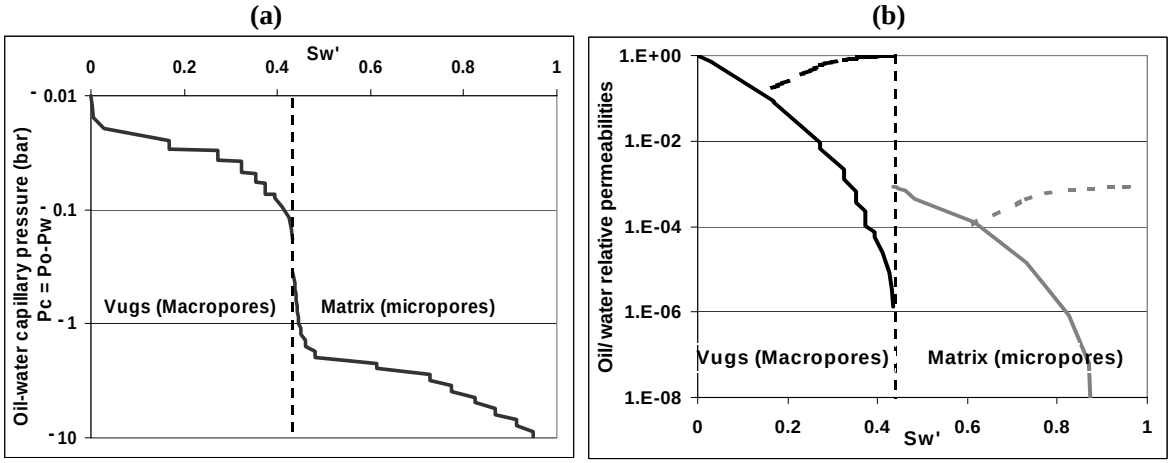

Figure 4. (a) Curves of capillary pressure and (b) relative permeability obtained for the matrix and the vugs network.

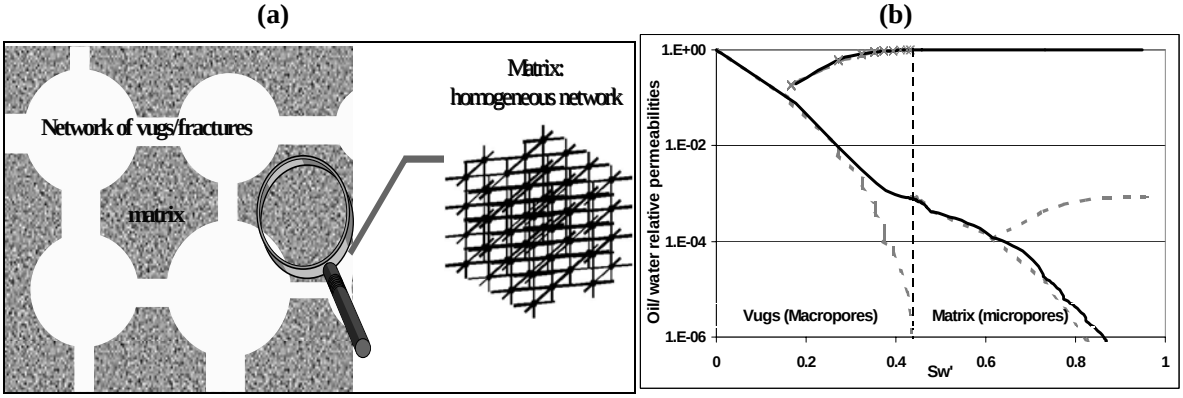

Figure 5. (a) Schematic description of a dual-network model. (b) Curves of relative permeability obtained for the dual-network (continuos lines), matrix and vugs are oil-wet.

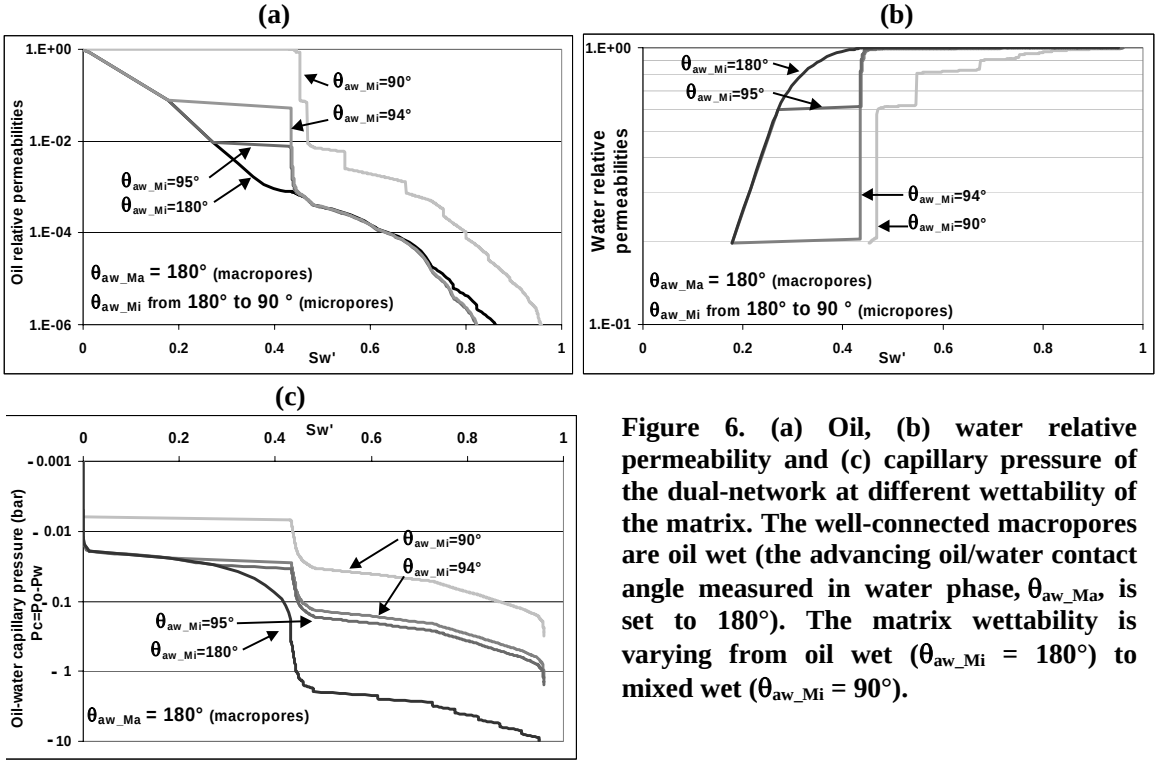

Figure 6. (a) Oil, (b) water relative permeability and (c) capillary pressure of the dual-network at different wettability of the matrix. The well-connected macropores are oil wet (the advancing oil/water contact angle measured in water phase, θ_{aw_Ma}, is set to 180°). The matrix wettability is varying from oil wet (θ_{aw_Mi} = 180°) to mixed wet (θ_{aw_Mi} = 90°).

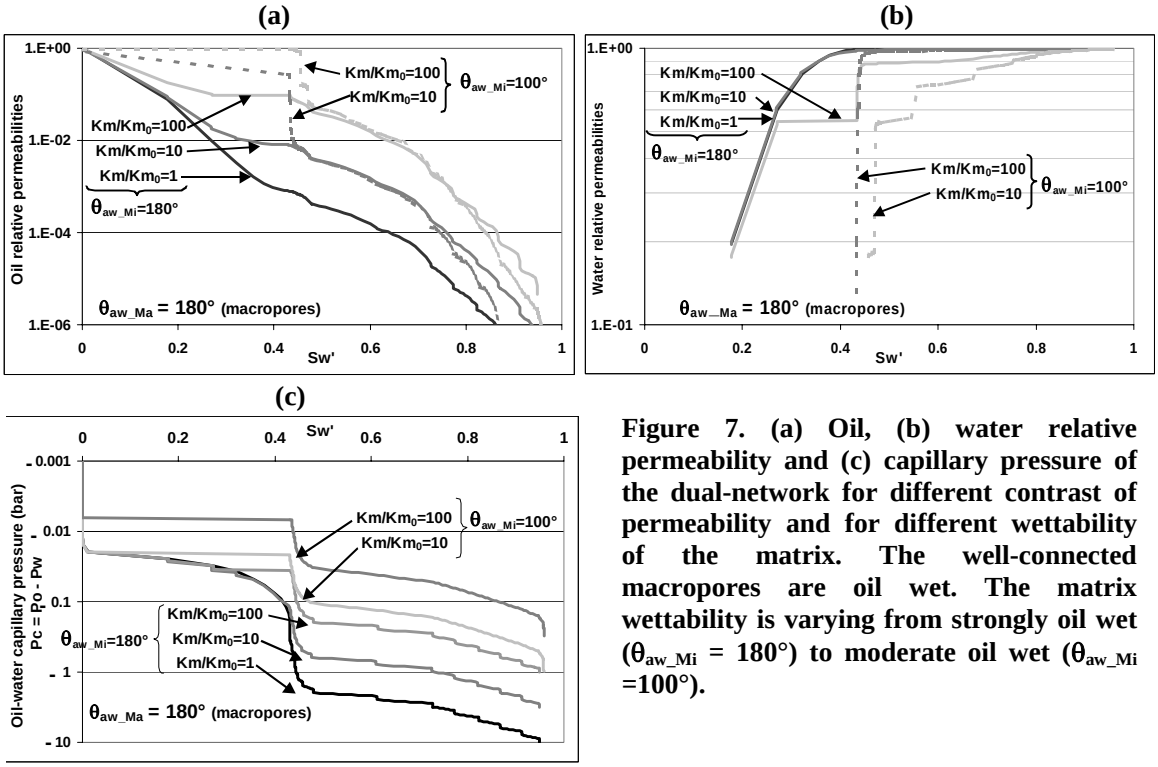

Figure 7. (a) Oil, (b) water relative permeability and (c) capillary pressure of the dual-network for different contrast of permeability and for different wettability of the matrix. The well-connected macropores are oil wet. The matrix wettability is varying from strongly oil wet (θ_{aw_Mi} = 180°) to moderate oil wet (θ_{aw_Mi} =100°).